PHOTONICS Research

High-quality 2-μm Q-switched pulsed solid-state lasers using spin-coating-coreduction approach synthesized Bi_2Te_3 topological insulators

Junpeng Qiao,[1] Shengzhi Zhao,[1,5] Kejian Yang,[1] Wei-Heng Song,[2] Wenchao Qiao,[1] Chung-Lung Wu,[2] Jia Zhao,[1] Guiqiu Li,[1] Dechun Li,[1] Tao Li,[1] Hong Liu,[3] and Chao-Kuei Lee[2,4,6]

[1]School of Information Science and Engineering, Shandong University, Jinan 250100, China
[2]Department of Photonics, Taiwan Sun Yat-sen University, 70 Lienhei Road, Kaohsiung 80424, China
[3]State Key Laboratory of Crystal Materials, Institute of Crystal Materials, Shandong University, Jinan 250100, China
[4]Research Center for Applied Sciences, Academia Sinica, 128 Sec. 2, Academic Road, Taipei 11529, China
[5]e-mail: shengzhi_zhao@sdu.edu.cn
[6]e-mail: chuckcklee@yahoo.com

Received 15 December 2017; revised 2 February 2018; accepted 2 February 2018; posted 2 February 2018 (Doc. ID 315809); published 27 March 2018

In this paper, the fabrication process and characterization of Bi_2Te_3 topological insulators (TIs) synthesized by the spin-coating-coreduction approach (SCCA) is reported. With this approach, high-uniformity nano-crystalline TI saturable absorbers (TISAs) with large-area uniformity and controllable thickness are prepared. By employing these prepared TIs with different thicknesses as SAs in 2-μm solid-state *Q*-switched lasers, thickness-dependent output powers and pulse durations of the laser pulses are obtained, and the result also exhibits stability and reliability. The shortest pulse duration is as short as 233 ns, and the corresponding clock amplitude jitter is around 2.1%, which is the shortest pulse duration in TISA-based *Q*-switched 2-μm lasers to the best of our knowledge. Moreover, in comparison with the TISA synthesized by the ultrasound-assisted liquid phase exfoliation (UALPE) method, the experimental results show that lasers with SCCA synthesized TISAs have higher output powers, shorter pulse durations, and higher pulse peak powers. Our work suggests that the SCCA synthesized TISAs could be used as potential SAs in pulsed lasers.

OCIS codes: (140.3540) Lasers, *Q*-switched; (160.4760) Optical properties.

https://doi.org/10.1364/PRJ.6.000314

1. INTRODUCTION

Nowadays, pulsed lasers emitting at the 2-μm wave band are gaining more and more attention for their wide application in the fields of medicine, interferometric sensing, coherent light detection and ranging, the manufacturing industry, as well as the pumping of optical parametric oscillators working at 3–5 or 8–12 μm [1–4]. Due to the advantages of flexibility, simplicity, compactness, and efficiency, passive *Q*-switching technique has been proved to be a favorable method to obtain laser sources from the visible to the middle-infrared (MIR) region [5–8]. With respect to the wavelength of 2 μm, various saturable absorbers (SAs), such as Cr:ZnSe [9], Pb-doped glass [10], InGaAs/GaAs [11], as well as carbon nanotubes (CNTs) [7] have been widely reported. These conventional SAs, however, have the problem of a narrow absorption band; in spite of that, those SAs have merits of flexible design of parameters, a large ratio of saturable to non-saturable losses, and a high damage threshold. For example, carbon nanotube (CNTs) have been widely investigated for their broad wavelength range, low cost, simple fabrication process, short recovery time (~1 ps), and high-speed third-order optical nonlinearity [7,12]. The cluster-induced losses and sample clarity also severely restrict their applications [13]. In the last few years, two-dimensional (2D) layered materials employed as SAs in mode-locked or *Q*-switched lasers have been broadly investigated and reported for their large nonlinearity and unique electronic band structure [14–22]. Since single- or few-layered graphene SAs were successfully applied in many kinds of mode-locked or *Q*-switched laser system [14,15], other kinds of 2D materials, such as black phosphorus (BP) [16,17], transition-metal dichalcogenides (TMDs) [18–20], and topological insulators (TIs) [21–28], have also received plenty of attention owing to their unique optoelectronic properties. When it comes to TIs, as reported in Ref. [21], a TI is also a Dirac material with a narrow topological non-trivial energy gap (0.16–0.3 eV) at its bulk state and a gapless metallic surface state. Just like graphene, due to the Pauli-blocking effect, the

saturable absorption of TI could happen when the TI is excited by strong light with the single photon energy exceeding the TI's bandgap. Benefiting from its advantages of narrow energy gap and gapless metallic state at its surface or edge, TI is expected to show an ultra-broad bandwidth of saturable absorption operation. Up to now, TIs have been employed as SAs in many mode-locked and *Q*-switched lasers from the visible to the near-infrared (NIR) range and show good performances [22–24]. With respect to a *Q*-switched 2-μm laser with TIs as SAs, several works on the TISA *Q*-switched 2-μm fiber lasers have been reported [25,26]; however, the reported pulse widths were more than 1 μs. Recently, our group has demonstrated a solid-state passively *Q*-switched 2-μm laser with a Bi_2Te_3-SA synthesized by ultrasound-assisted liquid phase exfoliation method (UALPE) [27], where the shortest pulse duration of 620 ns has been obtained. The 620 ns pulse duration was once the record of the pulse width for 2-μm *Q*-switched lasers with TIs as SAs. In this work, we have obtained 233 ns pulse width, which we think is the shortest one ever among the reported results of TISA *Q*-switched 2-μm lasers. To further improve performance, such as shortening the pulse duration for fulfilling requirement of applications, it is consequently expected to achieve narrow-pulse-duration 2-μm passively *Q*-switched lasers with TISAs of thickness or optical nonlinearity controllable 2D materials. To date, plenty of methods for preparing TISAs, such as the molecular beam epitaxy (MBE) and vapor–liquid–solid methods (VLS) [28], hydrothermal intercalation exfoliation (HIE) [29], liquid phase exfoliation (LPE) [30], the polyol methods [31], and the solvothermal methods [32], have been reported. In spite of the proved functionality of pulsing lasers with these methods, there are various drawbacks for each method. For example, the MBE and VLS are expensive and time-consuming. In HIE and LPE, it is hard to control the size of exfoliated nanostructure TIs and their samples' quality is limited by the bulk TI materials. As for the polyol and solvothermal methods, the aggregation of TI nanoplates depresses their application in pulsed lasers.

Recently, the spin coating-coreduction approach (SCCA) was discussed and reported for synthesizing Bi_2Te_3 SAs and pulsing *Q*-switched laser at 1 μm [33]. The SCCA can directly grow crystalline Bi_2Te_3 on a sapphire substrate without the transfer procedure of TI nanoflakes. The TISAs prepared through this method have consistency over a large area and a controllable thickness. In this work, the SCCA synthesized TISAs were used as SAs in a 2-μm *Q*-switched laser. For comparison, a passively *Q*-switched laser with a UALPE method synthesized Bi_2Te_3 SA is also investigated [27]. The *Q*-switched laser with SCCA synthesized TISAs can generate pulses with higher average output powers, shorter pulse durations, and higher pulse peak powers in comparison with the *Q*-switched laser with UALPE synthesized TISAs. This indicates that the SCCA synthesized TISAs have huge potential applications in high-quality *Q*-switched lasers.

2. PREPARATION AND CHARACTERIZATION OF Bi_2Te_3 TOPOLOGICAL INSULATORS

The process of SCCA used to prepare Bi_2Te_3 films is the same as the work reported in Ref. [34]. First, $Bi(NO_3)_3 \cdot 5H_2O$ and TeO_2 were dissolved in propylene glycol under stirring with a small amount of HNO_3 to obtain a transparent precursor mixture. Second, the transparent precursor solution was spin-coated on sapphire substrates to yield the precursor film and the precursor film was then dried on a hot plate to remove residual solvent. Finally, the TI film was prepared by heating the precursor film in a stainless-steel autoclave with a small amount of hydrazine hydrate as a deoxidizer. In this experiment, three pieces of TISAs with different concentrations of 0.012, 0.058, and 0.115 mol/L were prepared, which we named as TISA1, TISA2, and TISA3, respectively. Furthermore, a UALPE synthesized TISA sample named TISA4 was prepared for comparison with the SCCA synthesized TISAs.

Figure 1 shows the lateral dimensions and flake thicknesses of four TISAs which are measured by atomic force microscopy

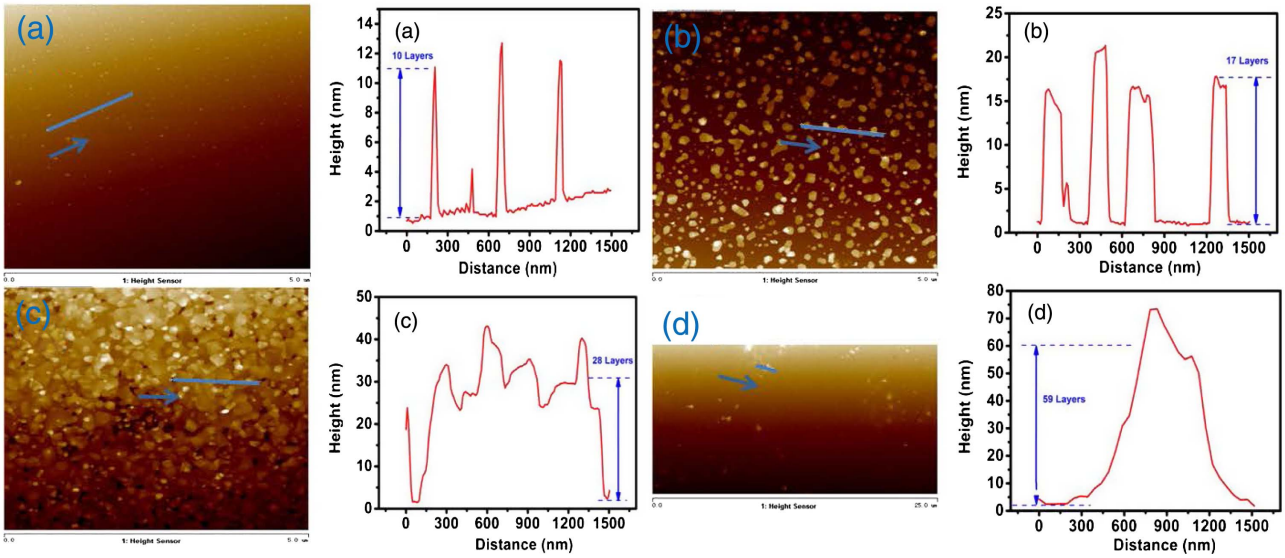

Fig. 1. AFM images and height variations of four TISAs. (a) TISA1; (b) TISA2; (c) TISA3; (d) TISA4.

(AFM). One should note that the scanning ranges are all 5 μm × 5 μm for TISA1, TISA2, and TISA3. As for TISA4, the scanning range of the AFM image is however 25 μm × 15 μm for clearly exhibiting its distribution. As shown in Fig. 1, the thicknesses of 10, 16, 27, and 57 nm are obtained for TISA1, TISA2, TISA3, and TISA4, respectively. Since the thickness of single layer TISA nanosheet is 0.96 nm [35], the layer numbers of these TISAs are estimated to be 10, 17, 28, and 59, respectively. Moreover, not only the thickness but also the coverage of the SCCA synthesized TISAs nanoflakes increases with the TIs' precursor concentrations, see Fig. 1. Additionally, compared with that of the UALPE method synthesized TISA, the uniformity of the SCCA synthesized TISAs nanoflakes is much better. In fact, one should note that the SCCA synthesized TISAs still exhibit good uniformity within even larger area, for example 1 cm × 1 cm, and the *Q*-switched solid state lasers at 1 μm using the SCCA synthesized TISAs as saturable absorber have been demonstrated and reported [34].

To investigate the nonlinear absorption properties of the prepared TISAs at 2 μm, the transmission after the TISAs with various input intensities was measured using 2-μm acousto-optically *Q*-switched laser with repetition rate of 100 kHz, pulse duration of around 300 ns and maximum output power of 1 W. The nonlinear transmittance curves versus input pulse influences are shown in Fig. 2. The nonsaturable loss of the SCCA synthesized TISAs shows the increasing trend with increasing values of TISA1, TISA2, and TISA3, 5.2%, 9.2%, 22.1%, respectively. In addition, the nonsaturable losses also increase as thickness of the TISAs and the corresponding modulation depths of TISAs from TISA1 to TISA3 can be estimated to be 6.7%, 11%, and 15%, respectively. Furthermore, the saturable intensities of TISAs from TISA1 to TISA3 are 0.8, 0.75, and 0.7 kW/cm^2, respectively. Hence, we can see that by adjusting the concentration of TIs, TISAs with different modulation depths can be obtained. This is due to that the decreasing surface-bulk coupling will slow down the relaxation of a generated photo carrier with increasing thickness of TIs [36,37]. This behavior also echoes the published work of the nonlinear absorption of the SAs at 1 μm [34]. As for the TISA4 sample, the nonsaturable loss, modulation depth, and saturable intensity are 7%, 16%, and 0.85 kW/cm^2, respectively.

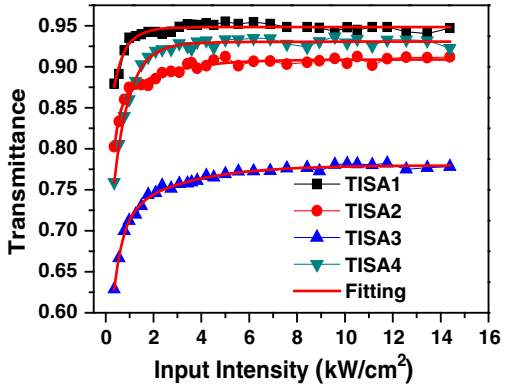

Fig. 2. Nonlinear transmittance curves versus input pulse influences.

3. *Q*-SWITCH OPERATION

To further investigate the saturable absorption properties of the as-prepared Bi_2Te_3 samples and their application feasibility for pulsed solid state lasers at 2 μm, a simple linear cavity solid-state laser test was used. The schematic experimental setup is shown in Fig. 3. A commercial fiber-coupled diode laser emitting at wavelength of 790 nm with a maximum output power of 50 W was used as the pump source. The fiber core with numerical aperture (NA) of 0.22 was 100 μm in diameter, and a 1:1 imaging module was employed to focus the pump light into the Tm:LuAG crystal. A 4 mm × 4 mm × 8 mm Czochralski-technique-grown Tm:LuAG coated with anti-reflection (AR) from 750 to 850 nm (reflectivity < 2%) and 1930 to 2230 nm (reflectivity < 0.8%) on both end sides was used as a laser crystal, and the Tm^{3+} ions' doping concentration was 6%. The crystal was wrapped with indium foils and held in a brass heat sink for efficiently cooling the laser crystal during pumping, and the temperature was held at 16 °C with a water cooler. As shown in Fig. 3, a mirror M_1 (r = 200 mm) was employed as the input mirror coated with high-reflection (HR) coating from 1850 to 2100 nm (reflectivity > 99.9%) and AR coating from 750 to 850 nm (reflectivity < 2%). Besides, a plane mirror M_2 was employed as output coupler (OC). For comparison, three OCs with different transmittances of 2%, 3%, and 5% from 1820 to 2100 nm were used. In this work, one UALPE synthesized TISA sample [27] and three SCCA synthesized TISAs were employed as the *Q*-switch SAs. The distance between M_1 and M_2 was about 20 mm. A digital oscilloscope (1 GHz bandwidth, Tektronix DPO 7102, USA) and a fast InGaAs photodetector with a rising time of 35 ps (EOT, ET-5000, USA) were used to measure the pulse characteristics of the laser. The spectrometer (resolution 0.4 nm, APE GmbH, Germany) and the power meter (Coherent Inc., USA) were employed to measure the laser spectrum and yielded average output power, respectively.

Figure 4 shows the average output power of *Q*-switched lasers with TISAs with respect to incident pump power and transmittances of OCs. Clearly, the thickness-dependent output can be seen with TISA1, TISA2, TISA3, and TISA4 for OCs with different transmittances of 2%, 3%, and 5%, respectively. The highest output powers for TISAs at the same incident pump power were obtained from the cavity with 5% transmittance of OC. In fact, as shown in Refs. [38,39], the output energy of passively *Q*-switched laser can be optimized by selecting an appropriate output coupler when the incident pump power, the gain medium, and the saturable absorber are given. Hence, the output power may be higher if the output coupler with transmittance more than 5% is employed. However, usually, to some extent, with the increase of output coupler transmittance, the *Q*-switched laser pulse will become

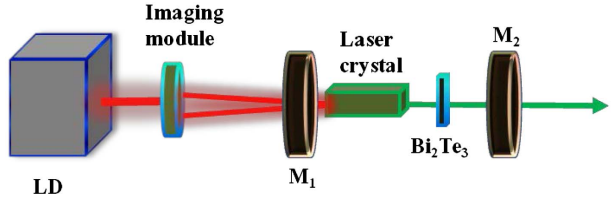

Fig. 3. Experimental setup of the *Q*-switched laser.

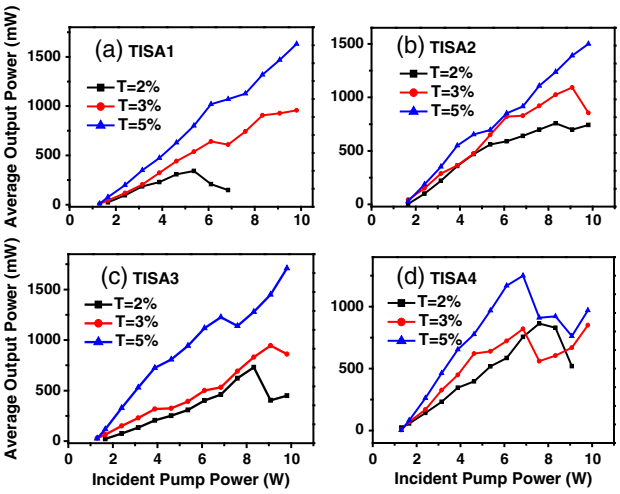

Fig. 4. Average output powers of Q-switched lasers with different TISAs and different OCs.

broad [39]. Therefore, in order to obtain Q-switched lasers with relatively short pulse widths, we chose three mirrors with relatively low transmittance. In addition, the power of Q-switched lasers with TISA4 reveals the reduction with increasing pump power further. Generally speaking, the thermal stability of saturable absorber is crucial for passively Q-switched laser operation [40]. The better thermal stability of SCCA synthesized TISAs is therefore expectable since TISAs synthesized by SCCA have better thermal conductivity resulting from the better uniformity in comparison to the UALPE synthesized TISAs.

From Figs. 4(a) to 4(c), we also can see that for output power of SCCA-based TISA Q-switched lasers with 5% output couplers there is no saturation tendency with the incident pump power increased to 10 W. However, saturation of output power occurs in the case of TISA4. Since we focus on the comparisons between the Q-switching performance of TISAs synthesized by different methods, we did not increase the incident pump power beyond 10 W, also in order to protect the gain medium from being damaged and avoid the thermal effect happening to the TISA due to the accumulation of excessive unabsorbed pump light.

Furthermore, as we can see from Figs. 4(a) and 4(c), the SCCA-based TI suffered from the output power decrease for the case of a 2% output coupling ratio. The reason may be as follows: for the Q-switched laser with 2% output coupling ratio, the power intensity inside the cavity is higher than that with 3% or 5% output coupling ratio. With the increase of the incident pump power, the high cavity power intensity will make the TI go from the normal state to the state of "over-saturation" due to the low saturation intensity of the TISA. At the state of "over-saturation," the accumulated heat on the TI sample causes an extra loss that makes the Q-switching laser performance deteriorated; hence, the output power will decrease [24]. However, even at the state of "over-saturation," we did not find damage to the TISAs. This is because the power intensity on SCCA-TISA in the cavity is about dozens of kilowatts per centimeter squared (kW/cm^2) in our experiment, while as reported in Ref. [41], at a power intensity of 26.7 MW/cm^2, the Bi_2Te_3-SA can still work without any damage. This indicates that the TISAs have a damage threshold larger than tens of megawatts per centimeter squared (MW/cm^2) and the related questions will be further investigated in future work.

In addition, the pulse durations and the repetition rates of these Q-switched lasers with 5% transmittance of OC versus incident pump powers are then analyzed and shown in Figs. 5(a) and 5(b). All are with clear pump power dependency. The highest power, highest repetition rate, and shortest pulse duration of the Q-switched laser using TISA4 as saturable absorber are close to the reported results and around 1.25 W, 98.5 kHz, and 671.2 ns, respectively [27]. In comparison to the laser using TISA4, however, the pulse durations and repetition rates using TISA1, TISA2, and TISA3 are with even better performance and clear thickness dependency. First, using incident pump power of 9.81 W, the shortest pulse durations for Q-switched lasers with TISA1, TISA2, and TISA3 are 435.4, 389.5, and 233.3 ns, respectively. The inset of Fig. 5(a) is the temporal profile of the shortest duration of the laser with TISA3 under pump power of 9.81 W. The decrease of the pulse duration could be attributed to higher modulation depth in the thicker TISAs [34]. Second, the laser pulse repetition rates become higher with increasing thickness of the TISAs. For example, the corresponding highest pulse repetition rates of TISA1, TISA2, and TISA3 are 105, 122, and 145.5 kHz, respectively, as shown in Fig. 5(b). These results all indicate that the SCCA synthesized TIs can be used as SAs with controllable nonlinear parameters for a pulsed laser.

Here, one should note that SCCA-based TISAs have an advantage of uniformity. As shown in Fig. 1, TISA4, grown by the UALPE approach, exhibits clearly uneven distribution, leading to extra thermal loss due to poor thermal dissipation efficiency as pumping goes higher. This can be used to explain why the output power of the Q-switched laser with TISA4 decreases

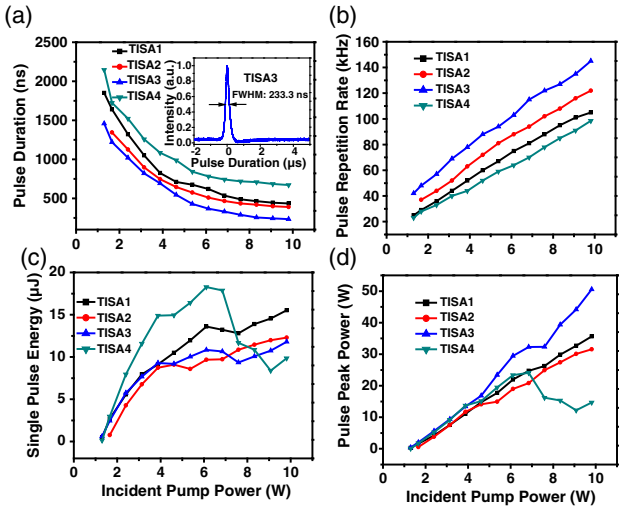

Fig. 5. Laser performances of Q-switched lasers with different TISAs versus incident pump powers. (a) Pulse durations; inset shows the temporal profile of the shortest duration of laser with TISA3 under pump power of 9.81 W; (b) pulse repetition rates; (c) single pulse energies; (d) pulse peak powers.

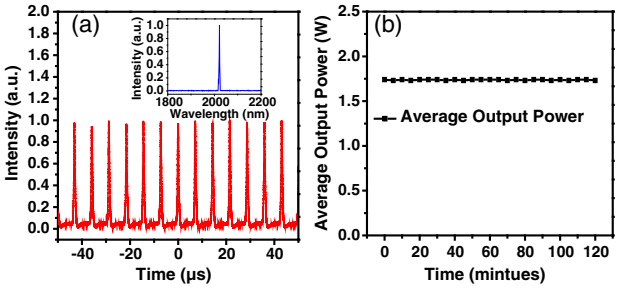

Fig. 6. (a) The pulse train of laser with TISA3 under pump power of 9.81 W, and the inset shows the corresponding spectrum; (b) stability of average output power of *Q*-switched laser with TISA3 at the incident pump power of 9.81 W.

when the incident pump power exceeds 7 W. Moreover, the pulse duration cannot be further depressed with increasing pump power. In contrast to TISA4, using SCCA-based TISAs, the output power increases monotonically with the increasing pump power. The pulse durations also decline accordingly with the increasing pump power. For example, as shown in Fig. 1(c), the SCCA-based TISA3 has more uniform TI flake distribution. Hence, its thermal dissipation efficiency is better than that of TISA4, and the problem of extra thermally induced loss is also relatively slight. Therefore, the SCCA-based TISA3 has better output power performance and shorter pulse width than TISA4. These all reveal SCCA-based TISAs have better potential for high power applications.

Furthermore, the single pulse energies and pulse peak powers can be estimated according to Eqs. (1) and (2),

$$E = P/f, \tag{1}$$

$$P_p = E/t, \tag{2}$$

where E, P, f, P_p, and t are the single pulse energy, the average output power, the pulse repetition rate, the peak power, and the pulse duration of the output laser, respectively. Figures 5(c) and 5(d) give the estimated pulse energies and the peak powers of *Q*-switched lasers with TISAs versus incident pump powers. The highest peak powers for TISAs from TISA1 to TISA4 are 35.6, 31.5, 50.5, and 24.1 W, respectively. For SCCA synthesized TISAs, the pulse peak power of laser with TISA3 is the highest among these TISA *Q*-switched lasers while the single pulse energy for a laser with TISA1 is higher than those of lasers with TISA2 and TISA3. This is because the laser with TISA3 has the shortest pulse duration.

In order to demonstrate the temporal quality of the pulses, the pulse train was characterized. Figure 6(a) shows one example of pulse train of laser with TISA3 as the absorber under a pump power of 9.81 W. The repetition rate is 145.5 kHz, and the pulse train is comparatively stable. We then evaluated the quality of pulse–amplitude equalization. This can be characterized by clock amplitude jitter (CAJ), which is defined as the ratio of the standard deviation (σ) to the mean value (M) of the intensity histogram at the pulse peak intensity, as in the following formula [29]:

$$\mathrm{CAJ} = \frac{\sigma}{M} \times 100\%. \tag{3}$$

The CAJ of the pulse train with the highest pulse energy (11.8 μJ) was calculated to be 2.1%, revealing good intensity stability. The inset of Fig. 6(a) is the corresponding optical spectrum and shows a clear emission wavelength of 2021.7 nm. In comparison with Ref. [27], there is a 3-dB optical bandwidth of the output pulse at the maximum power. This results from the introduced insertion losses induced by the SAs, in which the wavelength of a quasi-three energy level laser system will easily shift when switching the laser operation regime from continuous wave (CW) to *Q*-switching. Thus, if an extra element is employed in the cavity to vary the insertion loss, the central wavelength of the *Q*-switched laser would be tuned. In order to verify the sustainability of our laser system, the stability of average output power and pulse duration for a *Q*-switched laser with TISA3 at the incident pump power of 9.81 W was measured. We took the values every 5 min, and the whole measurement process lasted 2 h, as seen in Fig. 6(b). The average output power is around 1.74 W and with variation of about 10 mW. Clearly, within 2 h, the output powers of the lasers are within 1% variation. These all indicate the pulse quality of lasers using SCCA synthesized TISAs. Moreover, we compare the published works of 2-μm passively *Q*-switched lasers using

Table 1. Comparisons of 2-μm Passively *Q*-Switched Lasers with BP, MoS_2, WS_2, and Bi_2Te_3 SAs[a]

SA	Gain Medium	Wavelength	Output Power	Pump Efficiency	Pulse Width	Refs.
BP fiber	Tm^{3+}, Ho^{3+} fiber	1912 nm	71.7 mW	11.95%	731 ns	[16]
BP	Tm:YAP	1988 nm	151 mW	4.47%*	1.78 μs	[17]
BP	Tm:YAP	1969 nm and 1979 nm	3.1 W	41.2%*	181 ns	[42]
BP ceramic	Tm:YAG	2009 nm	38.5 mW	0.5%*	2.9 μs	[43]
MoS_2	Tm, Ho:YGG	2085 nm	206 mW	1.7%	410 ns	[19]
MoS_2	Tm:$GdVO_4$	1902 nm	100 mW	3.2%*	800 ns	[20]
MoS_2	Tm:CLNGG	1979 nm	62 mW	2.4%*	4.84 μs	[44]
MoS_2	Tm, Ho:YAP	2129 nm	399 mW	4.7%	435 ns	[45]
WS_2	Tm:LuAG	2013 nm	1.08 W	15.4%	660 ns	[46]
Bi_2Te_3	Tm^{3+}, Ho^{3+} fiber	1893 nm	0.68 mW	0.27%	1.71 μs	[25]
Bi_2Te_3 fiber	Tm^{3+} fiber	1957.6 nm	26 mW	3.3%	2.22 μs	[26]
Bi_2Te_3	Tm:LuAG	2023.6 nm	2.03 W	16.9%	620 ns	[27]
Bi_2Te_3	Tm:LuAG	2021.7 nm	1.74 W	17.7%	233 ns	This work

[a]The pump efficiency value with "*" at the top right corner represents the "output power/absorbed pump power," while the value without "*" represents the "output power/incident pump power."

2D materials as saturable absorbers, including BP, MoS_2, WS_2, and Bi_2Te_3. Table 1 shows the list of reported work about 2-μm *Q*-switched lasers. Except for Ref. [42], our work performs the shortest pulse duration and has relatively high output power among these *Q*-switched laser sources. One should note that the sustainability of the work of Ref. [42], which demonstrated a dual-wavelength laser with the highest output power of 3.1 W and the shortest pulse duration of 181 ns, is suspect due to BP materials' instability in air [47]. From the daily test of the pulse laser performance, the characteristics of the SCCA synthesized TISA-based pulsed laser are, however, with nearly fixed values under the same pump power. This also reveals the robustness of the SCCA synthesized TISA stored in the air. Therefore, we believe that the SCCA synthesized TISAs can be deemed as promising SAs in 2-μm solid-state pulsed lasers.

Previously, the difference of n and p type Bi_2Te_3 saturable absorption has been investigated [23]. By adjusting the density of the upper level for occupying as excitation through tuning the Fermi level, nonlinearity engineering was proposed for the pulsed laser. Unlike a typical semiconductor, however, it is not trivial for a topological insulator since the preparation of n or p type is difficult. Here, using the SCCA synthesized TISAs, the nonlinearity could be managed through adjusting the thickness of the TISAs resulting from dynamical modulation between bulk and surface state [34]. Besides, due to the TI's nature of broadband absorption, stable and reliable *Q*-switched solid-state lasers beyond 1 μm and 2 μm are also expectable. Moreover, the large area uniformity of the SCCA synthesized TISAs also makes the scaling from NIR to MIR *Q*-switched solid-state lasers possible due to their nature of high thermal conductivity and optical nonlinearity tenability.

4. CONCLUSION

In summary, by employing the SCCA method, scaling a 2-μm passively *Q*-switched solid-state laser with stable output was reported. This is due to the unique nature of the SCCA synthesized TISAs, which are of high-uniformity nano-crystalline within a large area and of controllable thickness. The laser performances of 2-μm solid-state passively *Q*-switched lasers with SCCA synthesized TISAs with different thicknesses are measured. At an incident pump power of 9.81 W, the shortest pulse duration of 233 ns is obtained, and the corresponding clock amplitude jitter is around 2.1%. As far as we know, this is the shortest pulse duration in a 2-μm passively *Q*-switched laser with a TISA. The most important issue is that scaling laser power becomes possible due to the better thermal conductivity of TISAs resulting from the better uniformity. Consequently, in comparison with the TISA synthesized by the UALPE method, the lasers with SCCA synthesized TISAs have higher output powers, shorter pulse durations, and higher pulse peak powers. All the experimental results indicate that the SCCA synthesized TISAs could be used as potential SAs in pulsed lasers.

Funding. National Natural Science Foundation of China (NSFC) (61775119, 61378022, 61475088, 61605100); Young Scholars Program of Shandong University (SDU) (2015WLJH38); Ministry of Science and Technology, Taiwan, China (MOST 106-2112-M-110-006-MY3).

REFERENCES

1. P. A. Budni, L. A. Pomeranz, M. L. Lemons, C. A. Miller, J. R. Mosto, and E. P. Chicklis, "Efficient mid-infrared laser using 1.9-μm-pumped Ho:YAG and $ZnGeP_2$ optical parametric oscillators," J. Opt. Soc. Am. B **17**, 723–728 (2000).
2. R. R. Gattass and E. Mazur, "Femtosecond laser micromachining in transparent materials," Nat. Photonics **2**, 219–225 (2008).
3. A. A. Lagatsky, S. Calvez, J. A. Gupta, V. E. Kisel, N. V. Kuleshov, C. T. A. Brown, M. D. Dawson, and W. Sibbett, "Broadly tunable femtosecond mode-locking in a Tm:KYW laser near 2 μm," Opt. Express **19**, 9995–10000 (2011).
4. G. Stoeppler, D. Parisi, M. Tonelli, and M. Eichhorn, "Tunable mid-infrared $ZnGeP_2$ RISTRA OPO pumped by periodically-poled Rb:KTP optical parametric master-oscillator power amplifier," Opt. Express **20**, 4509–4517 (2012).
5. R. Abe, J. Kojou, K. Masuda, and F. Kannari, "Cr^{4+}-doped $Y_3Al_5O_{12}$ as a saturable absorber for a Q-switched and mode-locked 639-nm Pr^{3+}-doped $LiYF_4$ laser," Appl. Phys. Express **6**, 032703 (2013).
6. H. Zhang, B. Ma, X. Chen, Q. Wang, X. Tao, and P. Li, "Passively Q-switched performance of a Nd:$Gd_3Ga_5O_{12}$ eye-safe laser at 1423.4 nm with Co^{2+}:$LaMgAl_{11}O_{19}$ as saturable absorber," Appl. Opt. **52**, 8576–8580 (2013).
7. J. Liu, Y. Wang, Z. Qu, and X. Fan, "2 μm passive Q-switched mode-locked Tm^{3+}:YAP laser with single-walled carbon nanotube absorber," Opt. Laser Technol. **44**, 960–962 (2012).
8. G. Zhu, X. Zhu, K. Balakrishnan, R. Norwood, and N. Peyghambarian, "Fe^{2+}:ZnSe and graphene Q-switched singly Ho^{3+}-doped ZBLAN fiber lasers at 3 μm," Opt. Mater. Express **3**, 1365–1377 (2013).
9. F. Qamar and T. King, "Passive Q-switching of the Tm-silica fiber laser near 2 μm by a Cr^{2+}:ZnSe saturable absorber crystal," Opt. Commun. **248**, 501–508 (2008).
10. M. Gaponenko, I. Denisov, V. Kisel, A. Malyarevich, A. Zhilin, A. Onushchenko, N. Kuleshov, and K. Yumashev, "Diode-pumped Tm:KY$(WO_4)_2$ laser passively Q-switched with PbS-doped glass," Appl. Phys. B **93**, 787–791 (2008).
11. B. Yao, Y. Tian, G. Li, and Y. Wang, "InGaAs/GaAs saturable absorber for diode-pumped passively Q-switched dual-wavelength Tm:YAP lasers," Opt. Express **18**, 13574–13579 (2010).
12. W. Cho, A. Schmidt, J. Yim, S. Choi, S. Lee, F. Rotermund, U. Griebner, G. Steinmeyer, V. Petrov, X. Mateos, M. Pujol, J. Carvajal, M. Aguilo, and F. Diaz, "Passive mode-locking of a Tm-doped bulk laser near 2 μm using a carbon nanotube saturable absorber," Opt. Express **17**, 11007–11012 (2009).
13. T. R. Schibli, K. Minoshima, H. Kataura, E. Itoga, N. Minami, S. Kazaoui, K. Miyashita, M. Tokumoto, and Y. Sakakibara, "Ultrashort pulse-generation by saturable absorber mirrors based on polymer-embedded carbon nanotubes," Opt. Express **13**, 8025–8031 (2005).
14. Q. Bao, H. Zhang, Y. Wang, Z. Ni, Y. Yan, Z. Shen, K. Loh, and D. Tang, "Atomic-layer graphene as a saturable absorber for ultrafast pulsed lasers," Adv. Funct. Mater. **19**, 3077–3083 (2009).
15. J. Xu, X. Li, Y. Wu, X. Hao, J. He, and K. Yang, "Graphene saturable absorber mirror for ultra-fast-pulse solid-state laser," Opt. Lett. **36**, 1948–1950 (2011).
16. H. Yu, X. Zheng, K. Yin, X. Cheng, and T. Jiang, "Nanosecond passively Q-switched thulium/holmium-doped fiber laser based on black phosphorus nanoplatelets," Opt. Mater. Express **6**, 603–609 (2016).
17. Z. Chu, J. Liu, Z. Guo, and H. Zhang, "2 μm passively Q-switched laser based on black phosphorus," Opt. Mater. Express **6**, 2374–2379 (2016).
18. G. Zhao, S. Han, A. Wang, Y. Wu, M. Zhao, Z. Wang, and X. Hao, ""Chemical weathering" exfoliation of atom-thick transition metal dichalcogenides and their ultrafast saturable absorption properties," Adv. Funct. Mater. **25**, 5292–5299 (2015).
19. S. Wang, H. Yu, H. Zhang, A. Wang, M. Zhao, Y. Chen, L. Mei, and J. Wang, "Broadband few-layer MoS_2 saturable absorbers," Adv. Mater. **26**, 3538–3544 (2014).
20. P. Ge, J. Liu, S. Jiang, Y. Xu, and B. Man, "Compact Q-switched 2 μm Tm:$GdVO_4$ laser with MoS_2 absorber," Photon. Res. **3**, 256–259 (2015).
21. H. Yu, H. Zhang, Y. Wang, C. Zhao, B. Wang, S. Wen, H. Zhang, and J. Wang, "Topological insulator as an optical modulator for pulsed solid-state lasers," Laser Photon. Rev. **7**, L77–L83 (2013).

22. Y. Cheng, J. Peng, B. Xu, H. Xu, Z. Cai, and J. Weng, "Passive Q-switching of Pr:$LiYF_4$ orange laser at 604 nm using topological insulators Bi_2Se_3 as saturable absorber," Opt. Laser Technol. **88**, 275–279 (2017).
23. Y. Lin, S. Lin, Y. Chi, C. Wu, C. Cheng, W. Tseng, J. He, C. Wu, C. Lee, and G. Lin, "Using n- and p-type Bi_2Te_3 topological insulator nanoparticles to enable controlled femtosecond mode-locking of fiber lasers," ACS Photon. **2**, 481–490 (2015).
24. Z. Luo, Y. Huang, J. Weng, H. Cheng, Z. Lin, B. Xu, Z. Cai, and H. Xu, "1.06 μm Q-switched ytterbium-dope fiber laser using few-layer topological insulator Bi_2Se_3 as a saturable absorber," Opt. Express **21**, 29516–29522 (2013).
25. J. Lee, M. Jung, J. Koo, C. Chi, and J. Lee, "Passively Q-switched 1.8-μm fiber laser using a bulk-structured Bi_2Te_3 topological insulator," IEEE J. Sel. Top. Quantum Electron. **21**, 0900206 (2015).
26. N. Muhammad Apandi, F. Ahmad, S. Zuikafly, M. Ibrahim, and S. Harun, "Bismuth telluride (Bi_2Te_3) topological insulator embed in PVA as passivle Q-switcher at 2 micron region," Photon. Lett. Pol. **8**, 101–103 (2016).
27. X. Liu, K. Yang, S. Zhao, T. Li, W. Qiao, H. Zhang, B. Zhang, J. He, J. Bian, L. Zheng, L. Su, and J. Xu, "High-power passively Q-switched 2 μm all-solid-state laser based on a Bi_2Te_3 saturable absorber," Photon. Res. **5**, 461–466 (2017).
28. Y. Guo, Z. Liu, and H. Peng, "A roadmap for controlled production of topological insulator nanostructures and thin films," Small **11**, 3290–3305 (2015).
29. Y. Lin, P. Lee, J. Xu, C. Wu, C. Chou, C. Tu, M. Chou, and C. Lee, "High-pulse-energy topological insulator Bi_2Te_3-based passive Q-switched solid-state laser," IEEE Photon. J. **8**, 1502710 (2016).
30. L. Sun, Z. Lin, J. Peng, J. Weng, Y. Huang, and Z. Luo, "Preparation of few-layer bismuth selenide by liquid-phase-exfoliation and its optical absorption properties," Sci. Rep. **4**, 4794 (2014).
31. B. Wang, H. Yu, H. Zhang, C. Zhao, S. Wen, H. Zhang, and J. Wang, "Topological insulator simultaneously Q-switched dual-wavelength Nd:Lu_2O_3 laser," IEEE Photon. J. **6**, 1501007 (2014).
32. Y. Sun, C. Lee, J. Xu, Z. Zhu, Y. Wang, S. Gao, H. Xia, Z. You, and C. Tu, "Passively Q-switched tri-wavelength Yb^{3+}:$GdAl_3(BO_3)_4$ solid-state laser with topological insulator Bi_2Te_3 as saturable absorber," Photon. Res. **3**, A97–A101 (2015).
33. P. Lee, Y. Sang, Y. Zhao, J. Xu, C. Tu, H. Liu, and C. Lee, "Preparation of few-layer bismuth telluride films by spin coating-coreduction approach (SCCA) and laser test," in *Lasers Congress 2016 (ASSL, LSC, LAC)* (Optical Society of America, 2016), paper AM5A.27.
34. Y. Wang, P. Lee, B. Zhang, Y. Sang, J. He, H. Liu, and C. Lee, "Optical nonlinearity engineering of a bismuth telluride saturable absorber and application of a pulsed solid state laser therein," Nanoscale **9**, 19100–19107 (2017).
35. Y. Sun, H. Cheng, S. Gao, Q. Liu, Z. Sun, C. Xiao, C. Wu, S. Wei, and Y. Xie, "Atomically thick bismuth selenide freestanding singly layers achieving enhanced thermoelctric energy harvesting," J. Am. Chem. Soc. **134**, 20294–20297 (2012).
36. J. Sobota, S. Yang, J. Analytis, Y. Chen, I. Fisher, P. Kirchmann, and Z. Shen, "Ultrafast optical excitation of a persisitent surface-state population in the topological insulator Bi_2Se_3," Phys. Rev. Lett. **108**, 117403 (2012).
37. Y. Glinka, S. Babakiray, T. Johnson, A. Bristow, M. Holcomb, and D. Lederman, "Direct optical coupling to an unoccupied dirac surface state in the topological insulator Bi_2Se_3," Appl. Phys. Lett. **103**, 151903 (2013).
38. J. Degnan, "Optimization of passively Q-switched lasers," IEEE J. Quantum Electron. **31**, 1890–1901 (1995).
39. J. Zayhowski and P. Kelley, "Optimization of Q-switched lasers," IEEE J. Quantum Electron. **27**, 2220–2225 (1991).
40. B. Chen, X. Zhang, K. Wu, H. Wang, J. Wang, and J. Chen, "Q-switched fiber laser based on transition metal dichalcogenides MoS_2, $MoSe_2$, WS_2, and WSe_2," Opt. Express **23**, 26723–26737 (2015).
41. P. Yan, R. Lin, S. Ruan, A. Liu, H. Chen, Y. Zheng, S. Chen, C. Guo, and J. Hu, "A practical topological insulator saturable absorber for mode-locked fiber laser," Sci. Rep. **5**, 8690 (2015).
42. H. Zhang, J. He, Z. Wang, J. Hou, B. Zhang, R. Zhao, K. Han, K. Yang, H. Nie, and X. Sun, "Dual-wavelength, passively Q-switched Tm:YAP laser with black phosphorus saturable absorber," Opt. Mater. Express **6**, 2328–2335 (2016).
43. Y. Xie, L. Kong, Z. Qin, G. Xie, and J. Zhang, "Black phosphorus-based saturable absorber for Q-switched Tm:YAG ceramic laser," Opt. Eng. **55**, 081307 (2016).
44. L. Kong, G. Xie, P. Yuan, L. Qian, S. Wang, H. Yu, and H. Zhang, "Passive Q-switching and Q-switched mode-locking operations of 2 μm Tm:CLNGG laser with MoS_2 saturable absorber mirror," Photon. Res. **3**, A47–A50 (2015).
45. C. Luan, X. Zhang, K. Yang, J. Zhao, S. Zhao, T. Li, W. Qiao, H. Chu, J. Qiao, J. Wang, L. Zheng, X. Xu, and J. Xu, "High-peak power passively Q-switched 2-μm laser with MoS_2 saturable absorber," IEEE J. Sel. Top. Quantum Electron. **23**, 1600105 (2017).
46. C. Luan, K. Yang, J. Zhao, S. Zhao, L. Song, T. Li, H. Chu, J. Qiao, C. Wang, Z. Li, S. Jiang, B. Man, and L. Zheng, "WS_2 as a saturable absorber for Q-switched 2 micron lasers," Opt. Lett. **41**, 3783–3786 (2016).
47. C. Wang, C. Zhang, C. Jiang, and T. Rabczuk, "The effects of vacancy and oxidation on black phosphorus nanoresonators," Nanotechnology **28**, 135202 (2017).